DOI: 10.30511/pcdp.2026.2082659.1061 - ISSN: 3060-8376 - Vol 3(3), 2026

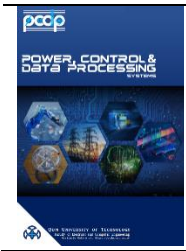

POWER, CONTROL AND DATA PROCESSING SYSTEMS

Available Online at: https://pcdp.qut.ac.ir/

A Voltage-Aware Operational Model for Active Distribution Networks with Energy Storage Systems

ARTICLE INFO

Article Type
Original Research

Authors
Javad Kazeman Seghin Sara[1]
Kamran Taghizad-Tavana[1,*]
Mohsen Ghanbari-Ghalehjoughi[1]
Hassan Niazi[1]
Mehrdad Tarafdar Hagh[1]

[1] Faculty of Electrical and Computer Engineering, University of Tabriz, Tabriz, Iran

**** Correspondence***
Address: 1Faculty of Electrical and Computer Engineering, University of Tabriz, Tabriz, , Iran,
Qom, Iran. Postal Code: 5166616471.
Phone: -
Fax: -
jkazeman@tabrizu.ac.ir
kamrantavana@tabrizu.ac.ir
mohsen.gnbr@gmail.com
hasan.nz@tabrizu.ac.ir
tarafdar@tabrizu.ac.ir

Article History
Received: December 31, 2025
Accepted: February 07, 2026
ePublished: September 01, 2026

ABSTRACT

This paper presents a voltage-aware operational framework for active distribution networks using a mixed-integer linearized optimization model. Unlike conventional approaches that treat voltage limits as hard constraints, a linear voltage deviation penalty is incorporated directly into the objective function, enabling voltage conditions to influence operational decisions, particularly the charging and discharging schedules of energy storage systems. The proposed formulation jointly considers active and reactive power dispatch, storage operation, and network losses within a single computationally tractable framework. Simulation results on the IEEE 33-bus distribution system demonstrate that the proposed approach leads to a smoother voltage profile at critical buses over the scheduling horizon, while maintaining voltages within acceptable limits. Compared to the base case, the total network losses are reduced from 3028.48 kW to 3027.66 kW, corresponding to a relative reduction of approximately 0.03%. In parallel, the modified objective function value reflects the explicit consideration of voltage quality, resulting in an increase of about 9.2% in the objective value, which represents a trade-off between voltage performance and operational cost. The results confirm that incorporating voltage deviation into the optimization objective enables voltage-aware storage operation and provides a transparent mechanism to evaluate its impact on network performance.

Keywords: Distribution system; Voltage-aware operation; Battery energy storage system; Renewable energy sources.

1 Introduction

1.1 . Motivation

The operation of distribution networks is increasingly influenced by the growing presence of energy storage systems and other distributed resources [1]. In this context, maintaining acceptable voltage levels remains a key technical requirement [2]. Most existing optimization-based scheduling approaches address voltage primarily through feasibility constraints or through separate voltage control mechanisms that are not directly coupled with economic scheduling decisions.
As a result, voltage deviations within allowable limits typically do not affect the optimization outcome, and their impact on the charging and discharging behavior of energy storage systems is not explicitly represented in the objective function [3]. This modeling choice limits the ability of existing frameworks to capture the interaction between voltage profile behavior, storage operation, and network losses in a unified manner. In practice, this interaction can be relevant, as operational decisions that are cost-effective may still lead to less desirable voltage profiles or higher losses.
This work is motivated by the need for an optimization framework in which voltage performance is directly reflected in operational decision-making. By incorporating voltage deviation into the objective function of a linearized mixed-integer model, the proposed approach allows voltage considerations to influence storage scheduling alongside conventional operational criteria. This enables a more consistent assessment of trade-offs between economic operation, voltage quality, and network losses within a single optimization model.

1.2 Literature review

In reference [4], the authors developed a multi-objective scheduling model for electric vehicles in power distribution networks, aiming to balance the economic interests of Electric Vehicle (EV) owners with the technical requirements of distribution network operators. The proposed framework simultaneously integrated Grid-to-Vehicle (G2V) and Vehicle-to-Grid (V2G) scheduling, battery health considerations, and hourly distribution network reconfiguration to reduce EV owners' costs, flatten the load profile, and improve overall network efficiency.
In reference [5], an operational framework for smart distribution networks was proposed, in which the spatio-temporal flexibility of data centers was coordinated with battery energy storage systems to reduce peak power exchange with the upstream network and minimize system losses. The study combined data center flexibility with battery storage operation under a robust optimization framework and employed sensitivity analysis to identify suitable installation locations, enabling improved management of renewable generation and load uncertainties. In this paper, voltage stability is investigated but not included in the objective function.
In reference [6], a bi-level optimization framework was presented for the planning, sizing, and placement of a vehicle refueling station supplied by renewable energy sources and battery systems within a smart distribution network. The framework jointly modeled infrastructure planning and operational scheduling, while incorporating reactive power management and uncertainty in demand, prices, and renewable generation through a stochastic optimization approach solved using Bender's decomposition.
In reference [7], an operational model for smart distribution networks was introduced that integrated demand response programs and battery energy storage systems to reduce power exchange with the sub-distribution substation. The proposed formulation accounted for battery degradation constraints, reactive power support from locally controllable generators, emission cost considerations, and uncertainty-aware optimization using box and polyhedral uncertainty sets. Also, in this article, open voltage stability is the main goal of the article, but it is not included in the main objective function.
In reference [8], a unit commitment formulation was developed that incorporated photovoltaic generation, battery energy storage systems, and power exchange with neighboring grids to improve the economic operation of the power system. A mixed-integer linear programming approach was employed to handle model nonlinearities and provide a flexible simulation framework supporting different linearization strategies and thermal unit configurations.
In reference [9], a real-time voltage control strategy for active distribution networks with high penetration of photovoltaic units and EV charging stations was presented. The study applied a time-decomposition-based dual-stage model predictive control framework with a reduced-order network model to coordinate reactive power resources and on-load tap changer operations, while limiting measurement and communication requirements and simultaneously addressing voltage regulation and energy loss minimization.
In reference [10], the limitations of conventional transmission-level network cost allocation methods when applied to transactive energy systems in distribution networks were investigated. The authors proposed a guideline for transactive energy operation that integrated physical network constraints with non-physical market characteristics to maintain network reliability. The applicability of the proposed approach was validated through numerical simulations under diverse network and market conditions.
In reference [11], renewable energy curtailment in active distribution networks caused by overgeneration, voltage violations, and line capacity constraints was examined. The study proposed the use of data centers as virtual batteries to provide spatiotemporal flexibility for shifting surplus renewable generation across time and locations. Simulation results on the IEEE 33-bus test system demonstrated significant reductions in renewable curtailment and power

supply costs, supported by sensitivity analysis on data center placement and uncertainty.

In reference [12], the increasing operational complexity of smart distribution networks was addressed by integrating demand-side and supply-side spatio-temporal flexibility. A coordinated framework was proposed that combined data centers for workload shifting with mobile storage systems as relocatable supply resources, supported by a risk-aware optimization model that accounted for uncertainty in renewable generation and load demand. In this paper, voltage stability is analyzed; however, it is not explicitly incorporated into the objective function.

1.3 Research Gap and Contribution

In many studies on the optimal operation of distribution networks, voltage is mainly considered as a feasibility constraint or handled through separate Volt/Var control mechanisms. Under these approaches, voltage deviations do not directly influence the economic scheduling of energy storage systems, and their effect on storage operation and network losses is not represented within a unified mixed-integer optimization framework. Consequently, the relationship between voltage performance and operational decisions remains insufficiently characterized.

This paper addresses this limitation by introducing a linear voltage deviation term into the objective function of a mixed-integer linearized distribution network model. With this formulation, voltage deviations are reflected in the optimization objective, allowing energy storage charging and discharging schedules to be influenced by voltage conditions alongside conventional operational criteria. This structure enables a consistent evaluation of the interaction between voltage profile behavior, storage operation, and total network losses within a single optimization model.

Table 1, presents the main gaps in the literature and the corresponding innovations proposed in this work.

References	Distribution network	Objective function			Renewable energy		Battery storage systems
		Cost	Losses	Voltage deviation penalty	WT	PV	
[4]	✓	✓	×	×	×		✓
[5]	✓	✓	✓	×	✓	✓	✓
[6]	✓	✓	×	×	✓	✓	×
[7]	✓	✓	✓	×	✓	✓	✓
[8]	✓	✓	×	×	×	✓	✓
[9]	✓	×	✓	×	×	✓	×
[10]	✓	✓	✓	×	×	×	×
[11]	✓	✓	✓	×	✓	✓	×
[12]	✓	✓	✓	×	✓	✓	✓
This work	✓	✓	✓	✓	✓	✓	✓

1.4 Paper structure

Section 2 describes the modeling approach and the mathematical formulation. Section 3 presents and analyzes the results. Section 4 concludes the paper and discusses limitations and possible directions for future work.

2 Mathematical Model

2.1 Objective Function

The objective function defined in (1) minimizes the total operational cost of the distribution network over the scheduling horizon. It consists of three components: the cost of energy purchased from the upstream grid, the cost associated with network active power losses, and a penalty term for voltage magnitude deviations.

The voltage deviation penalty is weighted by a coefficient of $\omega v = 120$, which enforces voltage regulation around the nominal value. The selected value of the voltage penalty coefficient was determined through empirical tuning to achieve a balanced trade-off between operational cost minimization and voltage regulation performance. The power loss cost is scaled by a unit loss coefficient $Cl = 1$. The energy purchasing cost is modeled using a piecewise-linear function whose incremental cost coefficients range from 0.1 to 1.3, allowing a gradual increase in marginal energy price. The energy purchasing term represents a monetary cost, whereas the voltage deviation term is dimensionless as it is defined in per-unit values. Accordingly, the voltage penalty coefficient is introduced to balance the relative impact of voltage regulation and operational cost in the objective function and was selected through empirical tuning.

$$Minobj = \sum_{h} Sc_h + \sum_{b,c,h} Cl\,(2bl_{b,c,h} - P_{b,c,h}^{Losses}) + \omega v \sum_{b,h} \left|\Delta_{b,h}^{Voltage}\right| \tag{1}$$

where the objective function consists of the substation energy purchasing cost, a loss-related penalty term, and a voltage deviation penalty. The voltage deviation penalty coefficient ω_v is introduced to balance the contribution of heterogeneous objective terms. While the substation energy cost is expressed in monetary units, the voltage deviation term is dimensionless as it is defined in per-unit values. Therefore, ω_v is required to ensure a meaningful trade-off between economic performance and voltage regulation. The selected value (ω_v = 120) was obtained through empirical tuning to effectively enforce voltage limits without dominating the economic objective under typical operating conditions. Within this range, the optimization results remain stable and preserve the intended trade-off between cost minimization and voltage performance.

The set of buses in the distribution network is denoted by I, with indices i and j. The set of time periods is denoted by T, indexed by t. All variables and constraints are defined over these sets unless otherwise stated. where all summations are explicitly defined over the sets of buses I and time periods T.

2.2 Active Power Balance Constraints

The active power balance at each non-slack bus is enforced by (2). This constraint ensures that, at every time period, the total active power generated by WT and PV units, combined with energy storage discharging, exactly balances the local active power demand, energy storage charging, and the net active power flowing through connected distribution lines.
For the slack bus, the active power balance is expressed by (3), where the active power exchanged with the upstream grid is explicitly included. The maximum allowable active power import from the upstream grid is limited to 5000 kW, ensuring realistic feeder capacity constraints.

$$P_{b,h}^{WindTurbine} + P_{b,h}^{Solar-Cell} - P_{b,h}^{ActiveDemand} + ES_{b,h}^{-} - ES_{b,h}^{+} = \sum_{c:r_{b,c}\neq 0} PT_{h,b,c}\, Non - SlackBuses(b \neq 1) \quad (2)$$

$$P_{b,h}^{WindTurbine} + P_{b,h}^{Solar-Cell} - P_{b,h}^{ActiveDemand} + ES_{b,h}^{-} - ES_{b,h}^{+} + P_{h}^{Substation} = \sum_{c:r_{b,c}\neq 0} PT_{h,b,c}\, SlackBuses(b = 1) \quad (3)$$

The hourly PV and WT generations profiles used in the simulations are presented in Fig. 1, which depicts the 24-hour power output patterns of renewable sources considered in this work. These time series are directly used as input data to represent the daily variability of PV and wind generation.

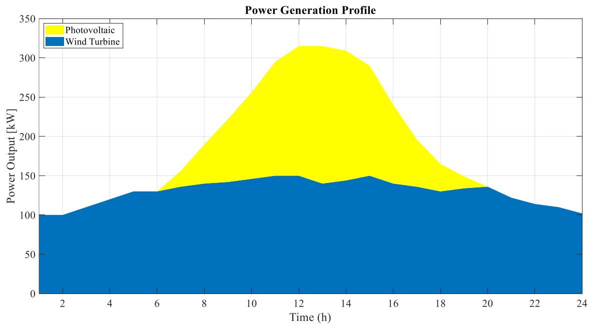

Fig.1. Renewable energy outputs [13, 14].

Regarding the hourly load profile, the spatial distribution of active and reactive power demands across the IEEE 33-bus network is illustrated in Fig. 2, which shows the nominal bus-wise load levels used in the study. The corresponding time-varying behavior of the system load is modeled using an hourly load profile applied to these nominal values, as described in the case-study section.
Uncertainty is not explicitly modeled in the numerical results presented in this paper, and all simulations are based on deterministic input profiles.

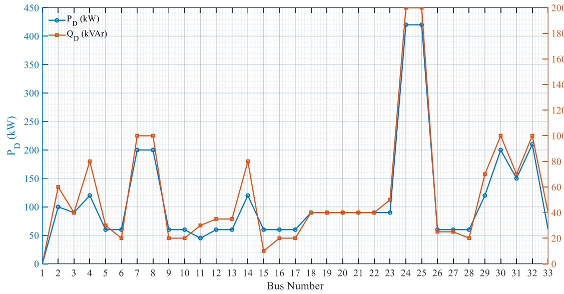

Fig.2. Hourly load profile.

2.3 Reactive Power Balance Constraints

Reactive power balance at non-slack buses is modeled by (4). At each bus, the reactive power demand is supplied by the network and, where available, by the reactive power capability of energy storage systems. For the slack bus, (5) incorporates the reactive power exchanged with the upstream grid. The maximum reactive power import is restricted to 2500 kVAr, reflecting the technical limits of the substation transformer and upstream network.

$$-Q_{b,h}^{Reactive\ Demand} + Q_{b,h}^{ElectricalStorage} = \sum_{c:r_{b,c}\neq 0} QT_{h,b,c}\, None - SlackBuses(b \neq 1) \quad (4)$$

$$-Q_{b,h}^{Reactive\ Demand} + Q_{b,h}^{ElectricalStorage} + Q_{h}^{Substation} = \sum_{c:r_{b,c}\neq 0} QT_{h,b,c}\, SlackBuses(b = 1) \quad (5)$$

2.4 Linearized AC Power Flow Equations

The linearized AC power flow model is defined by (6) and (7) [6, 15]. Equation (6) describes the active power flow of each distribution line as a function of voltage magnitude differences, voltage angle differences, and an approximated quadratic angle term. Equation (7) similarly represents the reactive power flow.
The conductance and susceptance of each line are derived from its resistance and reactance parameters. These parameters are computed based on the IEEE 33-bus distribution network data, ensuring accurate electrical representation of the system.

$$PT_{h,b,c} = \alpha_{b,c}(\Delta_{b,h}^{Voltage} - \Delta_{c,h}^{Voltage}) - \beta_{b,c}(\theta_{b,h} - \theta_{c,h}) + \frac{1}{2}\alpha_{b,c}\theta_{b,c,h}^{2} \quad (6)$$

$$QT_{h,b,c} = -\beta_{b,c}(\Delta_{b,h}^{Voltage} - \Delta_{c,h}^{Voltage}) - \alpha_{b,c}(\theta_{b,h} - \theta_{c,h}) - \frac{1}{2}\alpha_{b,c}\theta_{b,c,h}^{2} \quad (7)$$

The adopted linearized network model is reliable for typical operating conditions of distribution networks, where voltage magnitudes remain close to the nominal value and angle differences between adjacent buses are small. In this study, voltage deviations are explicitly constrained within a narrow range, which ensures the validity of the linear approximation.

2.5 Voltage Angle Linearization

2.5.1 Angle difference decomposition

To enable a linear optimization framework, the nonlinear voltage angle differences are approximated using a piecewise-linear approach. Equation (8) decomposes the voltage angle difference between two buses into positive and negative components. Equation (9) expresses the magnitude of the angle difference as the sum of auxiliary segment variables.

$$\theta_{b,h} - \theta_{c,h} = \theta^{+}_{b,c,h} - \theta^{-}_{b,c,h} \tag{8}$$

$$\theta^{+}_{b,c,h} - \theta^{-}_{b,c,h} = \sum_{y} \Delta\theta_{b,c,h,y} \tag{9}$$

2.5.2 Angle bounds

Constraints (10) and (11) bound the positive and negative angle components using a maximum allowable angle difference of 0.04 radians.

$$0 \le \theta^{+}_{b,c,h} \le \delta_{b,c,h}\theta^{max} \tag{10}$$

$$0 \le \theta^{-}_{b,c,h} \le (1 - \delta_{b,c,h})\theta^{max} \tag{11}$$

2.5.3 Piecewise angle segmentation

The piecewise segmentation logic is enforced through (12) – (14), where the angle range is divided into 20 equal segments.

$$For y = 1{:}\frac{\theta^{max}}{|y|_{b,c,h,1}{}_{b,c,h,1}\frac{\theta^{max}}{|y|}} \tag{12}$$

$$For 1 \le y \le |y|{:}\frac{\theta^{max}}{|y|_{b,c,h,y}{}_{b,c,h,y}\frac{\theta^{max}}{|y|_{b,c,h,y-1}}} \tag{13}$$

$$For y = |y|{:}\,\Delta\theta_{b,c,h,y} \le \frac{\theta^{max}}{|y|_{b,c,h,y-1}} \tag{14}$$

2.5.4 Quadratic angle approximation

Equation (15) reconstructs the squared angle term using a weighted summation of these segments, enabling an accurate linear approximation.

$$\theta^{2}_{b,c,h} = \sum_{y}^{\Sigma_{b,c,h,y}} (2y - 1)\frac{\theta^{max}}{|y|} \tag{15}$$

2.5.5 Voltage Magnitude Constraints

Voltage magnitude modeling is enforced by (16), where the bus voltage is expressed as a deviation from the nominal value of 1 p.u. Constraint (17) limits voltage deviations within the range of −0.1 to +0.1 p.u., ensuring compliance with standard distribution network voltage limits [16, 17]. The absolute value of voltage deviation is linearized by (18), allowing voltage deviations to be directly penalized in the objective function.

$$v_{b,h} = 1 + \Delta^{Voltage}_{b,h} \tag{16}$$

$$\underline{\Delta^{Voltage}} \le \Delta^{Voltage}_{b,h} \le \overline{\Delta^{Voltage}} \tag{17}$$

$$|\Delta^{Voltage}_{b,h}| \le d^{abs}_{b,h} \tag{18}$$

2.6 Substation Power and Cost Modeling

Substation power modeling is defined by (19) and (20). The total active power imported from the upstream grid is expressed as the sum of piecewise power segments, and the corresponding purchasing cost is calculated using predefined incremental cost coefficients. Constraints (21)–(23) enforce non-negativity and upper bounds on substation active and reactive power exchanges [18]. The parameter ψ represents the cost increment of each substation power segment and is set to 200. The maximum active and reactive power limits are set to 5000 kW and 2500 kVAr, respectively. Constraints (19)–(23) are enforced for all time periods h∈H and for all relevant indices.

$$P^{Substation}_{h} = \sum_{\sigma} \Delta P^{Substation}_{\sigma,h} \tag{19}$$

$$Sc_{h} = \sum_{\sigma} C_{\sigma}\, \Delta P^{Substation}_{\sigma,h} \tag{20}$$

$$0 \le \Delta P^{Substation}_{\sigma,h} \le \psi \tag{21}$$

$$0 \le P^{Substation}_{h} \le \overline{P^{Substation}_{h}} \tag{22}$$

$$0 \le Q^{Substation}_{h} \le \overline{Q^{Substation}_{h}} \tag{23}$$

2.7 Power Loss Modeling

Active power losses in the distribution network are modeled by (24) as the sum of bidirectional active power flows on each line. Constraint (25) ensures that the calculated power losses remain non-negative by introducing auxiliary loss variables, which are subsequently penalized in the objective function.

$$P^{Losses}_{b,c,h} = P_{b,c,h} + P_{c,b,h} \tag{24}$$

$$bl_{b,c,h} \ge P^{Losses}_{b,c,h} \tag{25}$$

Network losses are calculated based on the aggregated active power imbalance of line flows. Loss values are computed for each time period and reported in power units, and an aggregated loss index is obtained by summing the hourly values over the scheduling horizon.

2.8 Energy Storage System Constraints

2.8.1 SOC dynamics

The dynamic operation of energy storage systems is governed by (26) and (27) [19, 20]. Equation (26) initializes the state of charge (SOC) at the beginning of the scheduling horizon, while (27) updates the SOC for subsequent time periods based on charging and discharging actions.

$$For h = 1: SOC_{b,1} = \frac{\eta_b . ES^{+}_{i,1} . \Delta_h}{E_b} - \frac{\eta_b . ES^{-}_{i,1} . \Delta_h}{\eta_b E_b} \quad (26)$$

$$For h \geq 1: SOC_{b,h} = SOC_{b,h-1} \frac{\eta_b . ES^{+}_{i,1} . \Delta_h}{E_b} - \frac{\eta_b . ES^{-}_{i,1} . \Delta_h}{\eta_b E_b} \quad (27)$$

2.8.2 SOC limits

Each storage unit is characterized by a round-trip efficiency of 0.95 and an energy capacity of 700 kWh. The SOC of each storage unit is constrained between zero and its maximum allowable value, as enforced by (28) [21]. Constraint (29) ensures that the final SOC at the end of the scheduling horizon is not lower than a predefined threshold [22]. SOC evolution is modeled using an hourly time step, where charging and discharging powers are converted into stored energy based on the battery energy capacity. The SOC update explicitly accounts for the energy capacity of the storage system and the duration of each time interval.

$$\underline{SOC_b} \leq SOC_{b,h} \leq \overline{SOC_b} \quad (28)$$

$$SOC_{b,h} \geq \gamma \quad (29)$$

2.8.3 Charging/discharging exclusivity

Charging and discharging exclusivity is enforced by (30) and (31), preventing simultaneous charging and discharging of storage units [23-25]. The maximum charging and discharging power of each storage unit is limited to 250 kW. Charging and discharging efficiencies are explicitly incorporated into the SOC update equation, such that charging power is multiplied by the efficiency factor, while discharging power is divided by the same factor, reflecting realistic energy losses during battery operation.

$$ES^{+}_{i,h} \leq b^{ES}_{b,h} \overline{ES^{+}_{i}} \quad (30)$$

$$ES^{-}_{i,h} \leq (1 - b^{ES}_{b,h}) \eta_b \overline{ES^{+}_{i}} \quad (31)$$

2.8.4 Reactive power capability

Finally, (32) constrains the reactive power capability of energy storage systems within the range of −150 to +150 kVAr [26, 27].

$$\underline{Q^{ES}_b} \leq Q^{ES}_{b,h} \leq \overline{Q^{ES}_b} \quad (32)$$

All indices and summations are consistently defined throughout the formulation to ensure clarity and reproducibility.

In this work, voltage deviation is not modeled as an independent quantity detached from electrical variables. Instead, the voltage magnitude at each bus is represented through a deviation variable around the nominal value, and this deviation is explicitly coupled with network power flows via a linearized power-flow formulation. Specifically, the active and reactive power flows on each line are expressed as functions of voltage deviation differences between the incident buses and their voltage angle differences, using the line conductance and susceptance parameters derived from the network resistance and reactance data. In addition, nodal active and reactive power balance constraints are enforced at every bus and time period, linking the line flows to generation, demand, storage operation, and the substation power exchange. Therefore, voltage-related results are driven by the actual electrical quantities and network parameters within the adopted approximation. The use of this linearized representation is a deliberate modeling choice to preserve tractability and maintain a mixed-integer linear structure over the multi-period horizon, and it should be interpreted as an operationally consistent approximation rather than a full non-linear AC power-flow model.

3 Simulation Results

To evaluate the performance of the proposed voltage-aware operational framework, two case studies are conducted on the standard IEEE 33-bus distribution network. This test system is widely used as a benchmark in distribution network operation studies and includes distributed renewable generation, energy storage systems, and hourly load variations. Fig.3, shows a schematic diagram of a radial distribution feeder with distributed energy resources, including PV systems, WT, and battery energy storage units connected at different buses.

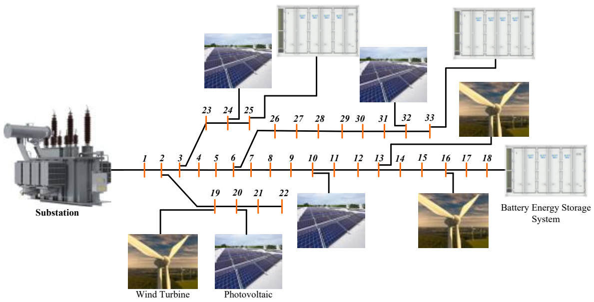

Fig.3. Schematic diagram of a radial distribution feeder with distributed energy resources, including PV, WT, and battery energy storage units connected at different buses.

The case studies are designed to isolate the impact of explicitly considering voltage deviation in the optimization objective

Case 1 (Base Case):

In this case, the distribution network is operated using conventional voltage constraints, while voltage deviation is not included in the objective function. The charging and discharging schedules of energy storage systems are determined based solely on economic considerations and standard operational constraints. This case serves as the reference scenario for comparison.

Case 2 (Proposed Case):

In this case, a linear voltage deviation penalty is added to the objective function. As a result, voltage conditions directly influence the optimization process, allowing energy storage systems to adjust their active and reactive power schedules in response to voltage deviations. This case is used to assess the effect of voltage-aware operation on voltage profiles, network losses, and the objective function value.

A comparative analysis of these two cases provides quantitative insight into how incorporating voltage deviation into the objective function influences operational decisions and system-level performance.

Fig. 4, presents the hourly voltage profiles of selected buses under the base case and the proposed strategy. The selected buses represent the slack bus, buses equipped with energy storage systems, and the end-of-feeder bus, allowing the evaluation of voltage behavior under reference, controlled, and worst-case conditions. The slack bus (Bus 1) maintains a constant voltage of 1 pu in both cases, indicating correct voltage reference modeling. At buses equipped with energy storage systems (Buses 18 and 25), the proposed strategy leads to slightly reduced voltage variations over time, particularly during higher load periods. At the end-of-feeder Bus 33, the minimum voltage magnitude remains nearly the same in both cases; however, the temporal voltage fluctuations are marginally lower under the proposed strategy. Overall, the results indicate that the proposed approach primarily reduces voltage variability rather than increasing voltage levels.

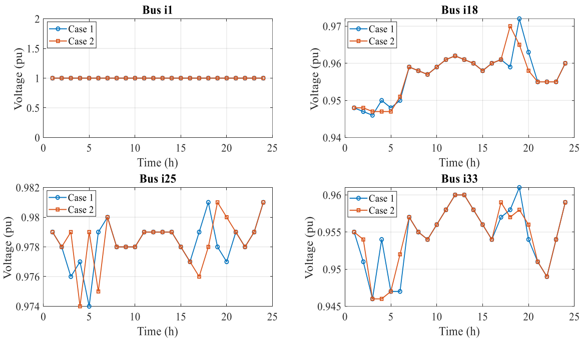

Fig.4. Hourly voltage profiles of selected buses in the distribution network for Case Study 1 and Case Study 2.

To quantitatively assess voltage profile improvement, system-wide voltage metrics are also evaluated. Specifically, the minimum and maximum bus voltages over the scheduling horizon, as well as the mean absolute deviation from the nominal value of 1 p.u., are calculated and reported.

Fig.5, compares the total network losses for case studies 1 and 2.

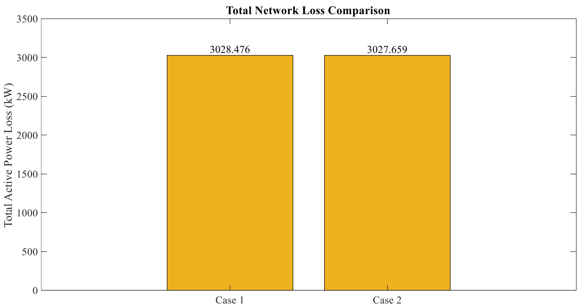

Fig.5. Comparison of total active power losses of the distribution network under Case Study 1 and Case Study 2.

Total network losses decrease from 3028.476 kW in the base case to 3027.659 kW under the proposed approach. Although the numerical reduction is limited, it reflects a more balanced power flow distribution across the network without altering load levels or network topology. This indicates that the proposed method improves operational efficiency by slightly reducing unnecessary line currents, which can contribute to energy savings over long-term operation.

As shown in Fig.6, the objective function value is higher in the proposed case compared to the base case. This increase is associated with the additional operational actions introduced by the proposed strategy. The result indicates a trade-off between operating cost and technical performance, where reduced network losses are achieved at the expense of a higher objective function value.

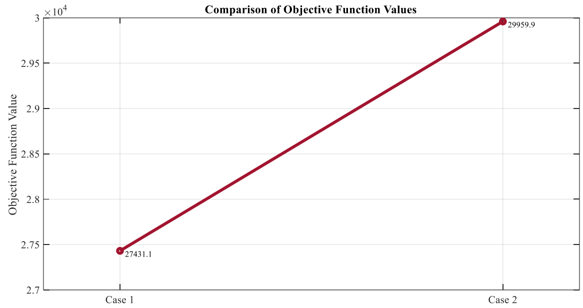

Fig. 6. Comparison of objective function values for Case Study 1 and Case Study 2.

Fig. 7, presents the 24-hour charging and discharging power profiles of the energy storage systems installed at buses i18, i25, and i33 for Case Studies 1 and 2. In both cases, charging occurs during hours 1–7 and discharging during hours 16–22, while zero power in the remaining hours indicates inactive periods.

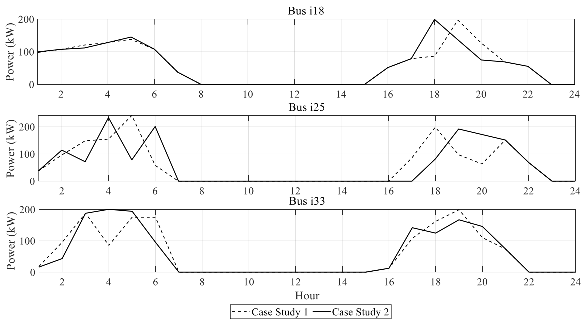

Fig.7. Comparison of 24-hour charging and discharging power of energy storage systems in Case Studies 1 and 2.

In Case Study 1, charging power is concentrated at bus i25, reaching approximately 242 kW at hour 5, whereas bus i33 charges at about 175 kW in the same hour. In Case Study 2, this distribution changes: at hour 5, the charging power of bus i25 decreases to about 78 kW, while the charging power of bus i33 increases to approximately 194 kW, and at hour 4 the charging power of bus i33 rises from about 86 kW to nearly 200 kW. During the discharging period, Case Study 1 shows higher output at bus i18 around hour 19 (approximately 197 kW), with lower contributions from bus i25. In contrast, Case Study 2 reallocates discharging power across the peak hours, as evidenced by the increase in discharging power at bus i18 from about 87 kW to approximately 199 kW at hour 18, and the increase at bus i25 to about 192 kW and 172 kW at hours 19 and 20, respectively. These numerical differences in Fig.7, indicate that Case Study 2 modifies the allocation of charging and discharging power among buses and peak hours, while maintaining the same operating time windows as Case Study 1.The observed improvement in these voltage metrics is mainly attributed to the coordinated charging and discharging behavior of the battery, which provides local voltage support during peak load and high renewable generation periods.

4 Conclusion

This paper presented a voltage-aware operational model for active distribution networks using a mixed-integer linearized optimization framework. In contrast to conventional formulations where voltage is enforced only through feasibility constraints, voltage deviation was included explicitly in the objective function via a linear penalty term. This formulation enabled voltage conditions to influence operational decisions, particularly the scheduling of energy storage systems, while preserving model solvability. Simulation results on the IEEE 33-bus distribution system showed that the proposed approach leads to a more uniform voltage profile at selected buses over the 24-hour horizon. Although voltage magnitudes in both the base and proposed cases remained within permissible limits, the proposed formulation reduced voltage variability during high-load periods. The observed changes in voltage behavior were associated with adjustments in the charging and discharging patterns of energy storage systems, indicating a coupling between voltage deviation and storage operation within the optimization process. In terms of network losses, the total losses decreased from 3028.48 kW to 3027.66 kW, corresponding to a reduction of approximately 0.03%. While the numerical magnitude of this reduction is limited, it indicates that voltage-aware operation can influence loss-related outcomes even when loss minimization is not the dominant objective. The results suggest that modifications in the temporal allocation of storage operation contribute to this effect. The objective function value increased by approximately 9.2% in the proposed case due to the explicit inclusion of voltage deviation. This outcome reflects the trade-off introduced by considering voltage quality alongside economic and operational criteria. The proposed framework therefore provides a structured means to evaluate the interaction between voltage performance, storage scheduling, and system-level metrics within a single optimization model.

Several limitations of this study should be noted. The use of linearized power flow equations improves computational tractability but may reduce accuracy under strongly nonlinear operating conditions. In addition, uncertainty in load demand and renewable generation was modeled in a simplified form, and detailed short-term voltage dynamics were not considered. The voltage penalty coefficient was assumed to be constant, and its sensitivity was not extensively analyzed.

Future work may include extending the formulation to multi-objective optimization, incorporating more detailed uncertainty representations, and investigating adaptive or time-dependent voltage penalty parameters. Applying the proposed approach to larger distribution networks and integrating additional voltage control devices may also provide further insight into its applicability.

AI Use Statement

AI tools were used solely to assist with English-language writing and editorial refinement.

Disclosure of Potential Conflicts of Interest

The Authors declare that there is no conflict of interest

Reference

[1] Lovro, L., A. Tomislav, and C. Tomislav, Changing the paradigm of distribution networks planning and operation: A systematic review of the distributed energy resources impact. Sustainable Energy, Grids and Networks, 2026. **45**: p. 102070.

[2] Keyu, Z., et al., Cooperative optimal operation of multi-microgrids and shared energy storage for voltage regulation of distribution networks based on improved Nash bargaining. International Journal of Electrical Power & Energy Systems, 2025. **166**: p. 110532.

[3] Fuchuan, D., et al., Voltage-variation-based adaptive virtual inertia control for dynamic power distribution in distributed energy storage battery system. Journal of Energy Storage, 2025. **132**: p. 117778.

[4] Subhadarshini, P. and G. Sanjib, Multi-objective smart charging scheduling scheme for EV integration and energy loss minimization in active distribution networks using mixed integer programming. Sustainable Energy, Grids and Networks, 2025. **43**: p. 101743.

[5] Kamran, T.-T., et al., Operation of smart distribution networks by considering the spatial–temporal flexibility of data centers and battery energy storage systems. Sustainable Cities and Society, 2024. **114**: p. 105746.

[6] Mehdi, V., Economic sizing and placement of hydrogen fueling and electric vehicles charging stations powered by renewable and battery systems in smart distribution network. Results in Engineering, 2025. **27**: p. 106657.

[7] Kamran, T.-T., et al., Multi-dimensional management of smart distribution networks: Comparative analysis of box and polyhedral methods for modeling uncertainties. Sustainable Cities and Society, 2024. **108**: p. 105488.

[8] Masoudi, M.R., M. Haghighi, and M. Rahimipour Behbahani, Optimal operation of solar energy system integrated with energy storage systems. Power, Control, and Data Processing Systems, 2024. **1**(1).

[9] Dar Mudaser, R. and G. Sanjib, Voltage regulation and energy loss minimization for distribution networks with high

photovoltaic penetration and EV charging stations using dual-stage model predictive control. Sustainable Energy, Grids and Networks, 2024. **40**: p. 101529.
[10] Noorfatima, N., J. Kong, and J. Jung, addressing challenges induced by transactive energy: Implications for network cost allocation policy in distribution systems. Renewable and Sustainable Energy Reviews, 2026. **230**: p. 116686.
[11] Abbas, et al., Application of robust optimized spatiotemporal load management of data centers for renewable curtailment mitigation. Renewable and Sustainable Energy Reviews, 2024. **204**: p. 114793.
[12] Hassan, N., T.-T. Kamran, and H. Mehrdad Tarafdar, Risk-constrained optimization of joint spatio-temporal flexibility of mobile energy storage and data centers under uncertainties in distribution systems. Energy Reports, 2025. **14**: p. 5072-5094.
[13] Ehsan, A., et al., Potential of environmentally friendly energy hubs with hydrogen and thermal storage devices on the voltage and temperature regulation in energy networks. Energy Conversion and Management: X, 2025. **28**: p. 101401.
[14] Mohammadali, N., et al., Flexibility pricing of integrated unit of electric spring and EVs parking in microgrids. Energy, 2022. **239**: p. 122080.
[15] Haojing, T., et al., DERs participation in TSO-DSO coordinated operation considering dynamic reconfiguration of distribution networks. International Journal of Electrical Power & Energy Systems, 2025. **173**: p. 111407.
[16] Brandon, C.-C., et al., A cost-effective integration and operation methodology for battery energy storage systems in active distribution networks via a master–slave optimization strategy. Journal of Energy Storage, 2025. **123**: p. 116639.
[17] Chaofan, H., et al., Renewable energy based low-voltage distribution network for dynamic voltage regulation. Results in Engineering, 2024. **21**: p. 101701.
[18] Shunxiang, Y., et al., Distributionally robust optimal scheduling of flexible distribution networks considering dynamic spatio-temporal correlation of renewable energy. International Journal of Electrical Power & Energy Systems, 2025. **169**: p. 110770.
[19] Ahhmadi, S. and M. Setayesh Nazar, Economic operation of multi-carrier microgrids considering energy markets and renewable electricity production. Power, Control, and Data Processing Systems, 2025. **2**(2): p. 53-60.
[20] Mohammad, S.-J., et al., Simultaneous planning of distribution automation and battery energy storage systems for improving resilience of distribution network. Sustainable Energy, Grids and Networks, 2025. **42**: p. 101709.
[21] Ping, D., et al., Research on multi-time-scale flexible operation method of distribution network considering deep reinforcement learning. International Journal of Electrical Power & Energy Systems, 2025. **172**: p. 111209.
[22] Haghighi, M., M.R. Masoudi, and M. Rahimipour Behbahani, Smart homes energy management system integrated with renewable energy sources and demand response programs. Power, Control, and Data Processing Systems, 2025. **2**(1): p. e719228.
[23] Nojavan, S., et al., Optimal demand response aggregation in wholesale electricity markets: Comparative analysis of polyhedral; ellipsoidal and box methods for modeling uncertainties. Heliyon, 2024. **10**(10).
[24] Md Masud, R., et al., Optimal sizing of battery storage for cost-effective peak shaving in regional distribution networks. Journal of Energy Storage, 2026. **141**: p. 119502.
[25] Bhattacharya, S., et al., Optimising the placement and sizing of a predefined number of battery energy storage systems on Distribution Networks. IFAC-PapersOnLine, 2024. **58**(13): p. 38-43.
[26] Wisam Najm Al-Din, A., Solving probabilistic optimal power flow with renewable energy sources in distribution networks using fire hawk optimizer. e-Prime - Advances in Electrical Engineering, Electronics and Energy, 2023. **6**: p. 100370.
[27] Ashraf Mohamed, H., et al., Impact of loading capability on optimal location of renewable energy systems distribution networks. Ain Shams Engineering Journal, 2024. **15**(1): p. 102340.